

The morphology of thermal cracks in brittle materials

Marianne Collin*, David Rowcliffe

Materials Science and Engineering, Royal Institute of Technology, SE-100 44 Stockholm, Sweden

Received 23 November 2000; received in revised form 28 March 2001; accepted 28 April 2001

Abstract

The geometry of indentation cracks propagated by quenching has been studied as a function of the severity of the quench. Practical results are obtained for alumina, silicon carbide whisker reinforced alumina and high speed steel. On quenching the crack growth is higher in the surface direction compared to the depth direction and an algorithm is suggested for calculating the crack depth from the measured surface crack length. The fracture mode in alumina differs between the indentation and the quench part of the crack and it is suggested that the stress intensity at the crack tip is one important parameter that determines the fracture path. When the stress intensity is close to the fracture toughness of the material, the fracture path is predominately intergranular while the fracture path is transgranular for higher levels of stress intensity. In the case of reinforced alumina the fracture path is transgranular through the matrix independent of the stress intensity. © 2002 Elsevier Science Ltd. All rights reserved.

Keywords: Al₂O₃; Crack growth; Indentation; Thermal shock resistance

1. Introduction

Materials that are used in high temperature applications are often exposed to rapid temperature changes which cause thermal stresses and risks for thermal shock damage. Examples are as varied as energy conversion systems, electronic devices and cutting tools. An indentation–quench test to evaluate the thermal shock resistance of brittle materials is currently being explored in detail.^{1–5} This test treats artificial cracks with known crack geometry, and as the cracks are made in the center of the sample, edge effects are avoided. The principal idea of the test is to study the growth of Vickers indentation cracks after quenching. The method is suitable both for evaluation of sequences of quenches with step-wise increasing temperature differences and repeated quenches with the same temperature difference (thermal cycling). The transient thermal stresses generated during quenching are normally tensile at the surface and compressive in the center of the body. For a single quench the thermal stress will first increase rapidly to a maximum value and then decrease more slowly to zero stress. In a recent analysis it was suggested that the stress pulse is long

enough to drive the crack to equilibrium and that the maximum level of tensile stress determines the crack growth.⁴ The level of tensile stress is highest at the surface and decreases with crack depth. This implies that for mild quenches the crack will only grow along the surface whereas after a certain critical quench, crack growth occurs also in the downward direction. An important result of this is that the crack shape after quenching changes from semicircular to semi-elliptical and that the crack depth is smaller than the surface crack length.^{3,4}

Previous papers have established that relatively light quenches cause stable crack growth (that is, the crack stops) whereas more severe quenches result in unstable growth.^{3,4} The regime with stable growth is due to the combination of thermal stress from the quenching and residual stress from the indent and the crack grows when the sum of thermal and residual stress exceeds a critical value. Thus the amount of thermal stress required for crack growth is lower when residual stress is present. In this way the presence of residual stress makes the indentation–quench test especially sensitive and allows the regimes of stable and unstable growth to be identified. These regimes can be predicted from changes in stress intensity when the crack size increases.⁴ For careful calculations of the stress intensity measures of both the surface crack length and the crack depth are needed. Measurement of the crack depth

* Corresponding author.

E-mail address: collin@met.kth.se (M. Collin).

demands fracturing the sample, which is often difficult. It would thus be valuable to have an algorithm which expresses the relation between the crack depth and the surface crack length. Hitherto no such algorithm has been suggested for indentation-quench cracks.

Indentation precracks have been used for other types of investigations, such as measurement of fracture toughness by combination of indentation and bending using the flaw-size method⁶ or the modified indentation technique.⁷ Also, in these cases the crack shape will change to semi-elliptical because the bending stress is highest at the surface.^{8–15} A common procedure to handle this effect is to evaluate changes in the crack shape and adjust the geometry factor in the expression used for the calculation of the fracture toughness. The crack shapes are evaluated either by measurement^{8,9,12–15} or by algorithms found in literature.^{10,11} According to one type of algorithm the crack shape a/c (where a is the crack depth and c is the surface crack length) is a function of the relation between the crack depth and the thickness of the bending bar (t) e.g. $a/c = 1 - a/t$ ¹⁰ and $a/c = 0.826 - 1.486 \times (a/t)$.¹¹ Some authors who have made measurements of the crack shape have suggested new algorithms, such as a linear decrease of a/c from 1 to 0.7 as c/c_0 changes from 1 to 2.5 (c_0 is the initial surface crack length)⁸ and a bilinear relation with an assumption that c increases at fixed a until $a/c = 0.75$ at which point a/c remains constant.¹³

Another important aspect of crack growth is the fracture path. The fracture path will be determined by a combination of the grain size, the relative strength of the grain boundary and the system conditions (e.g. the stress intensity at the tip of the crack, the crack velocity and the environment).^{16–20} Regarding the system conditions it is important to consider whether the crack is growing in a stabilizing field with decreasing crack velocity or in a destabilizing field with increasing crack velocity.²¹ In a destabilizing field the driving force on the crack increases away from equilibrium, while in a stabilizing field the driving force decreases towards equilibrium. This concept is particularly pertinent to the case of cracks subjected to quenches of differing severity. It is generally accepted that the crack velocity influences the fracture path in the way that a high crack velocity promotes transgranular crack growth.¹⁶ The effect of the velocity has indirectly been studied by varying the loading/unloading rate during indentation of fine-grained alumina^{22,23} and during stable crack growth during biaxial bending of indented bendbars.²⁴ It was shown that a very low loading rate (10^{-4} – 10^{-3} N/s) resulted in almost 100% intergranular fracture but when the loading rate was increased the contribution of transgranular crack growth increased. Similar investigations of the fracture path for thermal cracks are not known from the literature, but would give valuable information about crack growth during thermal load.

Thermal shock is characterized by a transient stress pulse. When indentation cracks are present, they propagate according to the severity of the quench and there is a transition from stable to unstable growth. For correct interpretation of results from the indentation–quench test, an increased knowledge about the crack propagation is essential. Thus, this paper focuses on the development of the crack and how the crack shape changes in different materials as a function of quench conditions. An expression for the crack depth as a function of the surface crack length is derived and the fracture paths for alumina and reinforced alumina are investigated. Further, the role of the residual stress is demonstrated by a practical experiment.

2. Materials and quenching experiments

2.1. Materials

Three different materials were investigated: (1) high-purity densely sintered fine-grained alumina with an average grain size $< 5 \mu\text{m}$, (Procera Sandvik), (2) alumina reinforced with 30 vol.% of silicon carbide whisker (Sandvik Coromant) and (3) high-alloy high speed steel, grade (ASP2060, Erasteel). The samples were in the form of plates (1) 13 mm diameter \times 4 mm, (2) 13 mm square \times 4 mm and (3) 15 mm diameter \times 4 mm. The high speed steel grade ASP2060 was chosen because radial cracks can be introduced by Vickers indentation. However, most high speed steel grades do not form such radial cracks during indentation.

2.2. Crack growth at the surface

The measurements were performed using the procedure previously established for the indentation-quench test.^{1,4} Precracks were made through indentation with a Vickers diamond for 20 s. The peak load and the mean crack size of the surface radial after indentation for each material were (1) 35 N and 114 μm , (2) 60 N and 102 μm , (3) 3000 N and 796 μm respectively. Approximately 20 indentation cracks were measured in each test. To evaluate the influence of residual stress, some indented samples of alumina were polished to remove 70 μm from the surface. In this way, both the indent and the plastic zone were removed. The remaining cracks had a mean surface crack length of 79 μm and a calculated crack depth of 35 μm . In addition, precracks were made in two reference alumina samples with the following peak loads and mean surface crack lengths: 35 N and 114 μm , and 12 N and 46 μm .

The quenches were made by heating the specimens in a furnace with air atmosphere and then quenching them by free fall into water at 30°C. The furnace temperature was selected to give the desired temperature difference,

ΔT , and ΔT -intervals of 20–40°C were chosen. The water bath did not show any measurable change in temperature during quenching. In all cases, the specimens were kept in the furnace for 20 min to assure temperature uniformity before quenching. In the main experiments, the same specimens were used in sequences of measurements with stepwise increasing temperature difference (requenched samples). In supplementary experiments alumina samples were repeatedly quenched (thermal cycling) with the same temperature difference ($\Delta T = 140^\circ\text{C}$).

2.3. Crack shape and fracture path

Crack shapes and fracture paths were investigated on cross-sections made by fracturing the samples in biaxial bending. The thickness of all samples but alumina was reduced to 2.5 mm by grinding the reverse side in order to get reasonable fracture loads. The cracks in alumina and reinforced alumina were colored with permanent ink before the fracture, while a weak oxidation of the crack surface that occurred during the heating and the quench steps made the cracks visible in high speed steel. Surface crack length and crack shapes were measured and investigated with an optical microscope. Investigation of fracture mode was made using a scanning electron microscope (JSM-840, Jeol Ltd., Tokyo, Japan).

3. Results and discussion

3.1. Crack growth at the surface

Fig. 1 shows the crack growth as a function of the temperature difference, ΔT , for thermal quenches of precracked samples of the three materials. The mean percentage surface crack length increase with respect to the as-indented surface crack length has been calculated from the growth of the individual cracks along the surface. The error bars show 95% confidence level. The pattern of crack growth is similar for all materials and can be divided into three regimes:

- Regime A. At very low ΔT , no significant crack growth can be detected.
- Regime B. In a medium ΔT interval, the crack growth is stable. The variation in percentage crack growth between the individual cracks is rather small as shown by the mean values at 95% confidence level. One reason for the scatter between the individual crack sizes is the variation in the microstructure at the tip of each crack. In the case of alumina and reinforced alumina, the cracks grow in a stepwise manner at the microstructural scale. This is illustrated in Fig. 2, which shows the growth of four individual cracks in reinforced

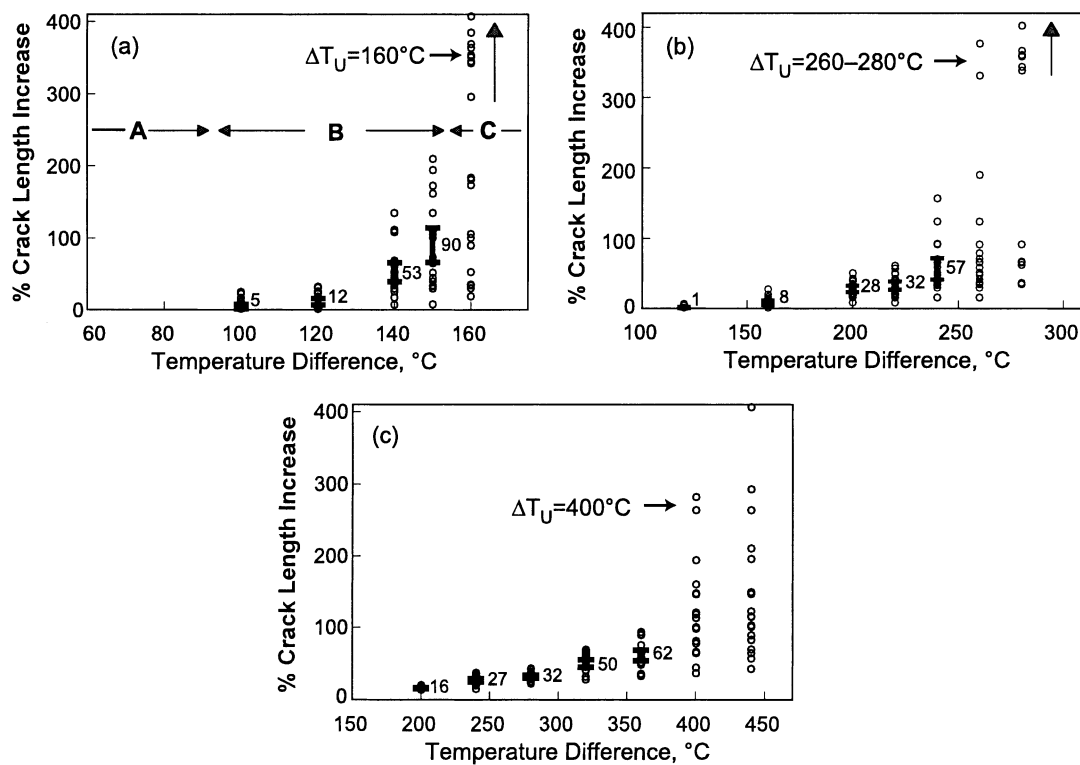


Fig. 1. Crack growth in indented (a) alumina, (b) reinforced alumina, and (c) high speed steel quenched over a range of temperature differences. The bars show 95% confidence level of the mean values.

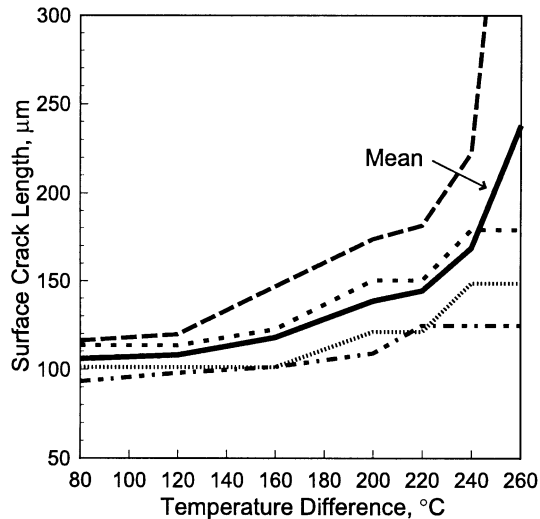


Fig. 2. Surface crack length of four individual cracks together with the mean surface crack length in reinforced alumina after quenching into 30°C water with stepwise increased temperature difference.

alumina together with the mean value. The cracks do not grow at every quench. A similar result has been reported for indentation-bending experiments.¹⁷

- Regime C. At a certain ΔT some of the cracks grow unstably out to the sample edge or stop at another indent, while the other cracks still grow stably or do not grow at all. The unstably grown cracks are rather large and it must be taken into account that stress can be relieved in the vicinity of these cracks. Consequently, as soon as one or more cracks have grown unstably, the amount of thermal stress will be decreased and those cracks that did not grow immediately have reduced possibilities to grow on further quenching. The temperature difference when Regime C starts is denoted as ΔT_U and the values are shown in Fig. 1. In the case of reinforced alumina two samples showed slightly different ΔT_U (260 and 280°C, respectively). Thus evaluation of crack growth at the surface shows the occurrence of regimes with stable and unstable crack growth in all three materials. These regimes are caused by the combination of residual stress from the indent and thermal stress from the quenching and have been modeled and explained elsewhere.⁴

The results in Fig. 1 were obtained by quenching the same sample with stepwise increasing temperature differences (requenched samples). Table 1 shows this result together with the result for a new sample quenched once with $\Delta T = 140^\circ\text{C}$. There is no significant difference. These results support the model of the indentation–quench test,⁴ which implies that the crack will grow as long as the stress intensity at the crack tip exceeds the fracture toughness of the material. Further the transient

Table 1

Quenching of alumina samples with different prehistory ($\Delta T = 140^\circ\text{C}$)

Prehistory of sample	Mean percentage crack growth (95% confidence interval)
Requenched sample 100–120–140°C	52.8 ± 13.1
New sample	34.9 ± 10.5

thermal stress pulse of one single quench is enough for the crack to reach its equilibrium during the stable crack growth regime and the maximum stress intensity is determined by the maximum stress during the quench. In this way the applied temperature difference will determine the crack growth independently of the prehistory of the sample on condition that the sample has not been quenched under more severe quenching conditions. This is advantageous for the indentation–quench test because more than one measurement can be made on one individual sample.

In another experiment, a new sample was quenched ten times with $\Delta T = 140^\circ\text{C}$ and the surface crack lengths were measured after one and 10 quenches. The results show that the crack growth between the first and the tenth quench is unevenly distributed among the cracks. Half of the cracks did not show any additional crack growth after the first quench while the others had grown significantly. Crack growth during thermal cycling of preindented samples has also been reported in the literature.^{2,25–27} The results in this work together with the information in the literature clearly show that stable crack growth can occur during thermal cycling. This kind of crack growth cannot be explained by the stress intensity concept referred to above,⁴ because according to this concept an increased crack growth demands an increased load as illustrated in Fig. 3 showing the total stress intensity at the surface versus the crack length. The total stress intensity after quenching is the sum of the residual stress intensity from the indent and the transient thermal stress intensity from the quench. The curves form minima because the residual stress intensity decreases and the thermal stress intensity increases with increasing crack length. Stable crack growth will only be observed when this stress intensity minimum is lower than the fracture toughness of the material as illustrated in Fig. 3 for $\Delta T = 140^\circ\text{C}$. In this case the crack growth along the surface will be stable until it reaches equilibrium and stops. When the thermal stress pulse has come to an end, the residual stress intensity is again the only contribution to the total stress intensity.

Crack growth during cyclic loading is often defined as fatigue. Compared to fatigue in metallic materials, there is very little research made on fatigue in ceramics and there is no generally accepted theory. There have been controversies about whether fatigue is due to slow crack

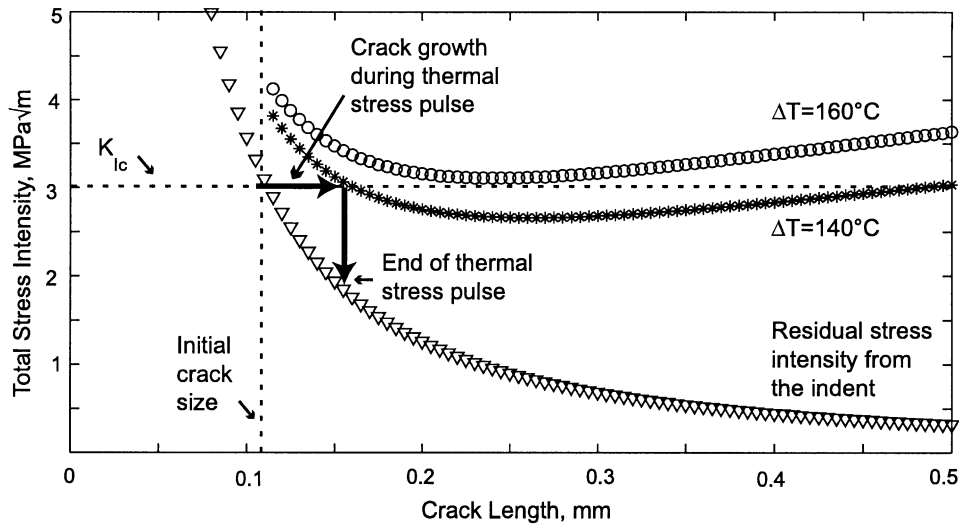


Fig. 3. Model of total stress intensity at the surface as a function of the crack length after quenching alumina with $\Delta T = 140^\circ\text{C}$ and $T = 160^\circ\text{C}$, respectively. The crack shape a/c is assumed to be 0.7. The figure also includes the residual stress intensity from the indent.

growth (stress–crack tip chemistry interaction) or if it is a “true” cycling effect.²⁸ Slow crack growth can occur when moist air and water is present at the same time as the stress intensity at the crack tip is high.¹⁸ For the indentation–quench test moist air is present during the indentation and the quenching is into water and therefore slow crack growth can occur if the stress intensity is high enough. The stress intensity, K , at the tip of a Vickers indentation crack can be estimated according to the following well-known relation:²⁹

$$K(c) = \frac{\chi P}{c^{3/2}} \quad (1)$$

Here, P is the indentation load, c is the crack size, and χ is called the residual stress factor and is a material dependent constant. After indentation, the stress intensity is at the critical value and slow crack growth can occur under the appropriate conditions. In this case, the stress intensity will decrease as the crack grows and approaches the threshold value for the material in the particular environment, when the crack ceases to grow. The maximum possible amount of slow crack growth depends on the material. In the case of the alumina grade used in this investigation it has been shown that there will not be any significant additional crack growth if an indented and measured sample is exposed to water for a period of 100 h. Thus, most of the possible slow crack growth has already occurred when the crack size is measured and is included in the initial surface crack length. After crack growth during quenching, the residual stress will be even lower according to Eq. (1) and slow crack growth between thermal cycles is improbable. Neither is slow crack growth probable during quenches because the stress pulse is very short.⁴ We thus have arguments to exclude slow crack growth as a possible

mechanism and suggest that thermal cycling crack growth is caused by a “true” cycling effect. It is reasonable to assume that fatigue effects during cycling of thermal loads and mechanical tensile loads are caused by similar mechanisms and that experience from mechanical fatigue in ceramics also is applicable for thermal fatigue. In a work covering fatigue in all types of material, it was pointed out that damage zones can develop ahead of cracks in ceramic materials subjected to tensile cycling loads due to retained permanent strains.³⁰ Another approach is that fatigue effects are connected to degradation of crack-tip shielding mechanisms.³¹ Crack growth during thermal cycling in brittle materials has been related to residual stress effects and microcracking due to thermal expansion anisotropy.^{27,32} Thermal cycling is a relatively unexplored research field and further investigations are needed in order to map out crack propagation in different materials and fatigue crack growth mechanisms. The indentation–quench test is an efficient method for this kind of research, because the test is well understood and it is easy to localize the cracks and measure the crack lengths.

3.2. Removal of indent before quenching

Fig. 4 shows the result after quenching of a sample from which the indent has been removed by polishing. The results are compared with two standard indented samples. One sample had a surface crack length the same as that of the original sample before the indent was removed. The other had a crack depth the same as the remaining crack depth after the indent was polished away. The results show that the sample, polished to remove the indent, has much lower crack growth compared to both the as-indented samples. This is due to the absence of residual stress in the polished sample and

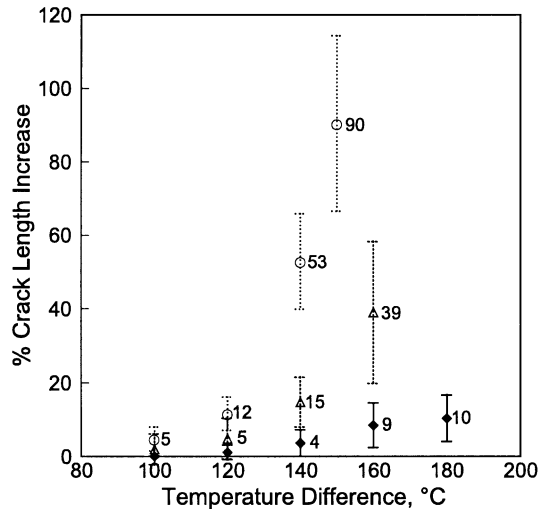


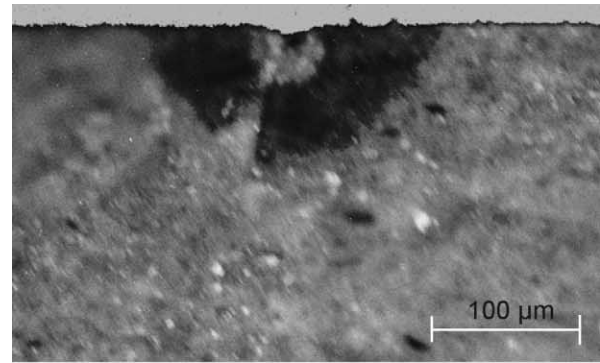
Fig. 4. Surface crack length in alumina polished to a depth of 70 μm (◆) together with non-polished references with a mean surface crack length of 114 μm (○) and 46 μm (△) after quenching into 30°C water with stepwise increased temperature difference. The bars show 95% confidence level of the mean values.

illustrates the important role residual stress plays in driving the cracks during quenching.⁴

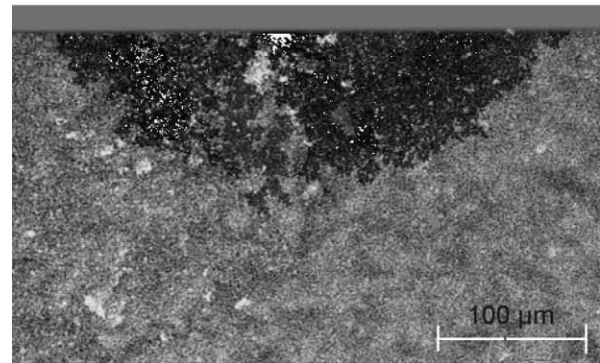
3.3. Subsurface crack shapes

Fig. 5 shows the crack shape in cross-section of reinforced alumina after indentation, indentation + quenching in the stable regime, and indentation + quenching in the unstable regime, respectively. The shape of the cracks after indentation is semi-circular whereas the shape changes to semi-elliptical after quenching in the stable regime. After quenching in the unstable regime the crack grows downwards to a depth of 1.4 mm and sideways to the edges of the sample. Similar crack shapes have been reported earlier for unreinforced alumina.³ The semi-elliptical crack shape is a consequence of the transient thermal stress generated during quenching being highest at the surface and decreasing with increasing depth.⁴ Thus, the stress intensity at the crack tip will be highest at the surface and the crack can grow in the surface direction at relatively mild quenches, while there is no growth in the downward direction. For crack growth in the downward direction, more severe quenches are needed. The reason for the crack to stop growing at a certain crack depth in the unstable regime is that the transient thermal stresses are compressive in the center of the plate as has been shown by FEM calculations.⁴

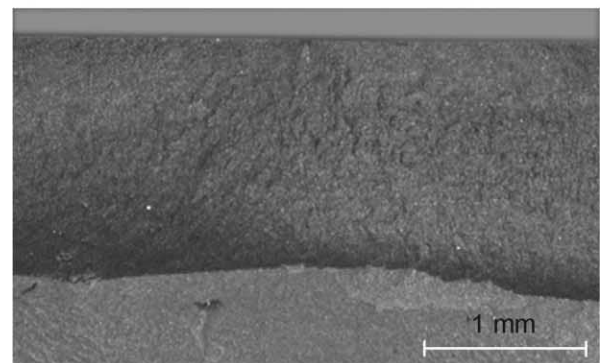
Cross-sections of cracks in high speed steel after quenching in the stable and unstable regimes are shown in Fig. 6. The darkest parts of the cracks show the crack shape after heating in the furnace. This is believed to represent the original indentation crack, the surface of which is revealed by mild oxidation during the furnace treatment. After quenching in the stable regime the



(a)



(b)



(c)

Fig. 5. Cross-sections in reinforced alumina showing crack shapes; (a) as indented sample; (b) after quenching with $\Delta T = 240^\circ\text{C}$; (c) after quenching with $\Delta T = 280^\circ\text{C}$.

cracks grow preferentially at the surface and almost only in the direction away from the indent. After quenching in the unstable regime the crack grows to a depth of about 0.9 mm. It is important to notice that the material closely below the indent has not been oxidized and has not been penetrated by the crack. After indentation the material in this zone is under compressive stresses, which stop the crack from growing into the zone during quenching. The crack passes through the compressive zone during the later mechanical fracture of the specimen accomplished in order to reveal the cross-section.

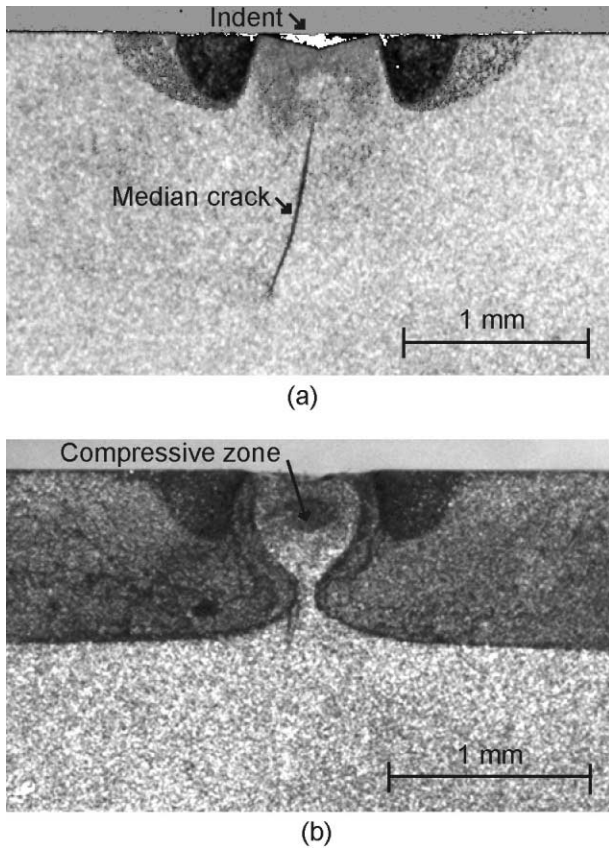


Fig. 6. Cross-sections in high speed steel showing crack shapes; (a) after quenching with $\Delta T = 320^\circ\text{C}$; (b) after quenching with $\Delta T = 440^\circ\text{C}$.

Approximate calculations of thermal stress intensity can be made using surface crack length alone. However, the above information on change of crack shape during quenching can be used to derive more accurate values of stress intensity along the crack front, leading to a more reliable prediction of thermal failure during quenching. A convenient way to express the crack shape is the shape factor, a/c , which shows the relation between the crack depth, a , and the surface crack length, c . Fig. 7 shows the shape factor measured for alumina and reinforced alumina as a function of the surface crack length. The shape factor seems to be a bilinear function of the surface crack length and there seems to be a breakpoint at $a/c = 0.7$. As mentioned above the crack growth in the downward direction is negligible for mild quenches. Based on these facts it is suggested that the crack depth, a , can be calculated according to the following algorithm:

$$\begin{cases} a = c_0, & c_0 < c < 1.4c_0 \\ a = 0.7c, & 1.4c_0 < c < 2.5c_0 \end{cases} \quad (2)$$

Here, c_0 is the initial surface crack length and c is the actual surface crack length. This algorithm is included in Fig. 7. It is similar to an algorithm in the literature for indentation + bending suggesting the breakpoint to be $a/c = 0.75$.¹³ Eq. (2) will be a good approximation for

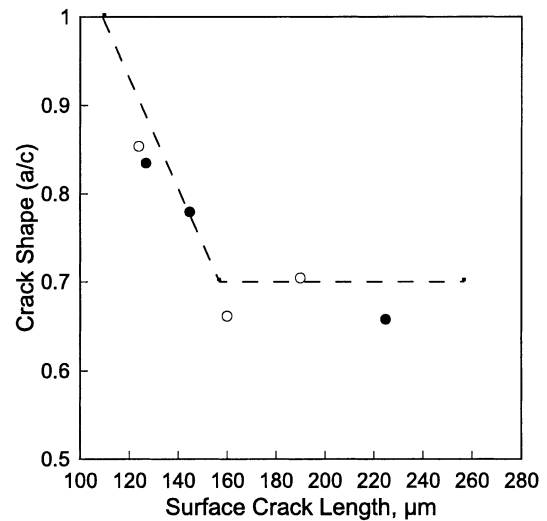


Fig. 7. Crack shape, a/c , as function of surface crack length, c , in unreinforced (○) and reinforced alumina (●) together with Eq. (2) (---).

all indentation–quench systems with a semi-circular precrack and a Biot number in the range 1–5, which is characteristic for the quenching conditions used in this investigation.⁴ In the case of higher or lower Biot numbers, the breakpoint has to be calibrated. For precracks with other crack shapes, a new investigation has to be made.

Specifically the crack depth (a_U) at the onset of unstable crack growth is important because it is used in an expression for prediction of ΔT_U and thermal shock resistance.⁴ In the literature, it has been proposed that the surface crack length at the onset of unstable crack growth is 2.5 times the initial surface crack length when an indent is exposed to tensile load.⁶ Using Eq. (2), a_U can be calculated to be $2.5 \times 0.7 c_0 \approx 1.75 c_0$, where c_0 is the initial surface crack length.

3.4. Fracture path

Fig. 8 shows a cross-section of an alumina sample which has been indented and quenched at $\Delta T = 160^\circ\text{C}$ and thereafter fractured in biaxial bending. Only the part of the crack which originates from indentation and quenching will be considered in this paper. As illustrated in Fig. 8a the indentation part of the crack is semicircular. On quenching, the crack grows to the edges in the surface direction and downwards to a depth of about 1.3 mm.³ Based on a reported analysis of the growth of indented cracks at quenching⁴ it is assumed that the quench crack has grown stably in a zone close to the indentation crack and unstably outside this zone.

The fracture path of the indentation crack is intergranular in a zone ($\approx 30 \mu\text{m}$ deep) directly below the indent as illustrated in Fig. 8b. This is in agreement with results reported earlier.²³ It has been reported that the zone immediately below the indent is characterized by compressive stresses and that the indentation crack

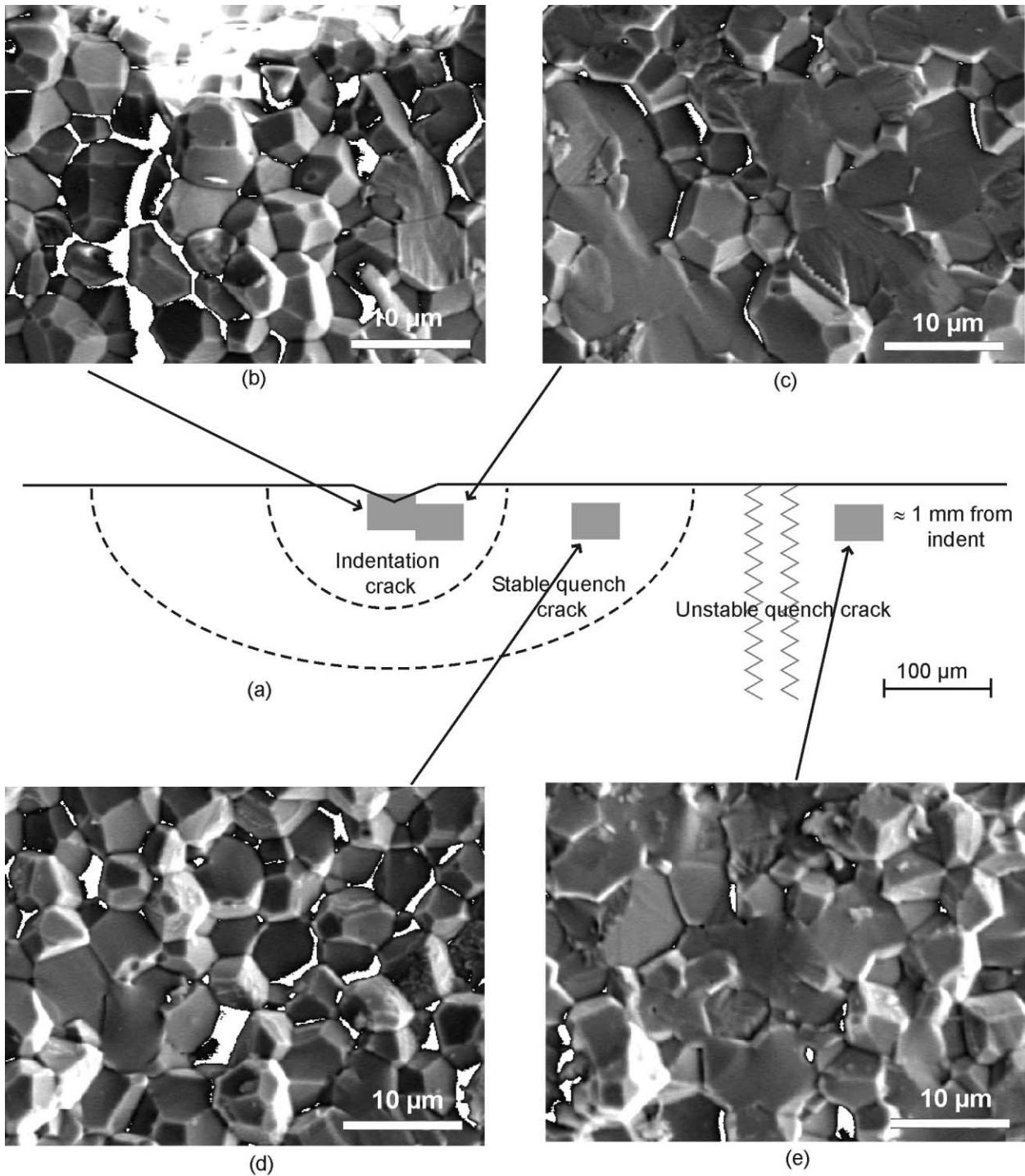


Fig. 8. Cross-section in alumina after quenching with $\Delta T = 160^\circ\text{C}$; (a) schematic drawing; (b) fracture surface of the zone below the indent characterized by compressive stresses after indentation; (c) fracture surface of indentation crack; (d) fracture surface of stably grown quench crack; (e) fracture surface of unstably grown quench crack.

cannot grow into it. The fracture of this compressive stress zone most likely occurred at the fracturing of the sample after the quenching in the same way as suggested for high speed steel (Section 3.3). The indentation crack shows a dominating transgranular fracture mode, as shown in Fig. 8c. At the rim of the indentation crack the fracture mode is once again intergranular (not shown).

This appearance of the indentation crack agrees with earlier reported results for an indentation crack with a loading/unloading rate (10 N/s) comparable to the rate used in this investigation (3.5 N/s).³³ The fracture path of the stably grown quench crack is predominantly intergranular (Fig. 8d), while the amount of transgranular fracture is higher in the unstably grown zone (Fig. 8e).

If the fracture resistance in the grain boundary and in the grain had the same level the crack would always choose the shortest way and the fracture path would always be transgranular. The occurrence of intergranular fracture indicates that the fracture toughness of the grain boundary is lower than that of the grain and that it is energetically favorable for the crack to choose the longer way around the grains.^{17,20,34} As already mentioned, it has been shown that a low loading rate promotes intergranular fracture while the contribution of transgranular fracture increases at higher loading rates. There is, however, no known thorough explanation of why the crack only chooses the longer way around the grains at low loading rates.

It is worthwhile to notice that the amount of intergranular fracture is higher in the stable quench part of the crack compared to the indentation part. This is surprising because it has been suggested that the amount of transgranular fracture increases with the loading rate.^{22,23} The estimated loading time for a quenched crack is about 6×10^{-2} s,⁴ which is much shorter than the loading/unloading time for the indentation (10 s) and reasonably the loading rate is much higher for quenching compared to indentation. A conclusion from this result is that any comparison of the loading rate between different loading systems should be made with care. The loading rate seems not to be the key property determining the fracture mode and we should look for another model to explain the results. It is well accepted that the mechanical energy release rate (qualitatively equivalent to the stress intensity at the crack tip) influences the crack velocity in reactive environments.^{18,21} It is thus reasonable to assume that the stress intensity could influence the fracture mode. An advantage of using the stress intensity is that the magnitude of it can be estimated. According to Eq. (1) the stress intensity at the tip of an indentation crack will decrease when the crack grows and approach the fracture toughness of the material when the crack ceases to grow. In the case of quenching of an indented sample, the stress intensity at the crack tip equals the fracture toughness of the material as the crack starts to grow and it will remain close to this value as the crack grows stably because the residual contribution to the total stress intensity will decrease and the thermal stress contribution will increase when the crack size increases. The unstable growth will occur in a destabilizing field and the stress intensity at the crack tip will increase with increasing crack size. If we put together the information about the fracture mode for alumina and the stress intensity, it can be seen that the fracture mode is predominantly transgranular when the stress intensity is high as in the indentation zone and in the unstably grown quench zone, while the fracture turns to more intergranular when the stress intensity is closer to the fracture toughness of alumina as at the rim of the indent and in the zone with stable growth after

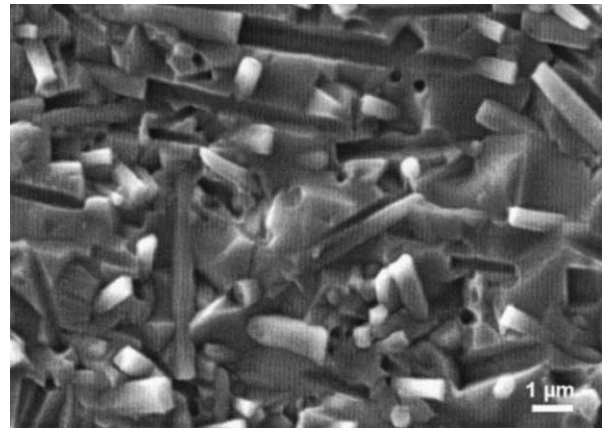


Fig. 9. Fracture surface of reinforced alumina after quenching with $\Delta T = 280^\circ\text{C}$. The appearance with transgranular fracture through the matrix and protruding whiskers as well as grooves is characteristic for both the indentation and the quench part of the crack.

quenching. It thus seems reasonable that the stress intensity is an important parameter in determining the fracture mode.

Similar investigations of the fracture path on a cross-section of the indentation and the quench part of the crack have been made for reinforced alumina quenched with $\Delta T = 280^\circ\text{C}$. In contrast to unreinforced alumina, reinforced alumina shows the same type of fracture path on all parts of the crack. Fig. 9 shows a characteristic appearance of the fracture surface for reinforced alumina. The fracture mode is transgranular through the matrix. In addition the fracture surface is characterized by protruding whiskers and grooves showing that whiskers have been pulled out. This is in agreement with results reported in the literature for precracked bend bars.³⁵ According to a model presented recently, the mechanism for crack growth in silicon carbide whisker reinforced alumina is completely different from that of unreinforced alumina.³⁶ First, the whiskers put the alumina matrix in tension. Second, the whiskers take an active part in increasing the energy needed for the crack growth by elastic bridging, frictional bridging and pullout bridging. It is reasonable to assume that both the tensile stress field and the active role of the whiskers overrule any fracture resistance differences between the grain boundaries and the grain bulk, and that the overall stress state in combination with the whisker distribution determines the fracture path.

It is worth noticing that the fracture modes for unreinforced and reinforced alumina are very different, but in the indentation–quench test the materials show the same type of growth pattern with a transition from stable to unstable crack growth. This supports the contention that the indentation–quench test is a reliable method that can be applied to most brittle materials. The usefulness of the method for different types of brittle materials is also illustrated by the results for high speed steel.

4. Summary and conclusions

The indentation–quench test technique has been studied with focus on changes in the crack shape and the fracture mode. Results on alumina and silicon carbide whisker reinforced alumina show that the crack shape is changed from semicircular after indentation to semi-elliptical after stable crack growth due to quenching. This is because the generated transient thermal stress is highest at the surface. An algorithm is suggested for calculating the crack depth from the measured surface crack length. This expression is valuable for careful calculation of thermal stress intensity at the crack tip. After unstable crack growth the crack shape is almost linear and extends to the edges in the surface direction and stops at a given crack depth because of the transient compressive stresses in the middle of the sample.

Indented and quenched samples of alumina and reinforced alumina were fractured and it was shown that the fracture modes differ distinctly. For alumina, the part of the crack that originates from the indentation shows predominantly transgranular fracture with an intergranular rim. The stably grown quench crack shows predominantly intergranular fracture while the amount of transgranular fracture increases in the zone where the crack has grown unstably. It is suggested that the stress intensity at the crack tip is one important parameter that determines the fracture mode. The fracture mode in reinforced alumina is transgranular through the matrix and the fracture surface is characterized by protruding whiskers and grooves showing that whiskers have been pulled out. This appearance is characteristic both for the indentation zone, the stable quench zone and the unstable quench zone. The crack shape after indentation and quenching has also been studied for relatively brittle high speed steel. The crack shape is radial after indentation, elongated in the surface direction after the stable quench growth and almost linear after the unstable quench growth in a comparable way to the crack shapes of alumina and reinforced alumina. This suggests that the indentation–quench test can be used for most brittle materials on condition that it is possible to introduce an indentation precrack.

Results in this paper show that the same sample can be used for repeated quenches on condition that the earlier quenches are made at a lower or at the same temperature difference. Repeated quench experiments at the same temperature difference (thermal cycling) for alumina showed a significant crack growth. The mechanisms for this is not clear but could be due to generation of a damage zone ahead of the crack or degrading of crack-tip shielding mechanisms. Further studies in this field involving more materials would give more knowledge concerning the mechanisms and the growth rates. The indentation–quench test is an efficient method for this kind of research, because the test is well understood and

it is easy to localize the cracks and measure the crack lengths. Information about thermal cycling resistance would be a valuable complement to the thermal shock resistance for candidate materials to applications characterized of repeated rapid temperature changes.

Acknowledgements

This work has been performed within the center for Inorganic Interfacial Engineering, supported by the Swedish National Board for Industrial and Technical Development (NUTEK) and the following industrial partners: Erasteel Kloster AB, Ericsson Cables AB, Höganäs AB, Kanthal AB, OFCON AB, Sandvik AB, Seco Tools AB and Uniroc AB.

References

- Andersson, T. and Rowcliffe, D., Indentation thermal shock test for ceramics. *J. Am. Ceram. Soc.*, 1996, **79**(6), 1509–1514.
- Andersson, T. and Rowcliffe, D., Thermal cycling of indented ceramic materials. *J. Eur. Ceram. Soc.*, 1998, **18**(14), 2065–2071.
- Collin, M. and Rowcliffe, D., Analysis of the indentation–quench test for ceramics. *Ceram. Eng. Sci. Proc.*, 1999, **30**(3), 301–308.
- Collin, M. and Rowcliffe, D., Analysis and prediction of thermal shock in brittle materials. *Acta Mater.*, 2000, **48**, 1655–1665.
- Collin, M. and Rowcliffe, D., Prediction of thermal shock resistance of components using the indentation–quench test. In *Proc. 7th Int. Symp. Ceramic Materials and Components for Engines*, Goslar, Germany, ed. J. G. Heinrich and F. Aldinger. Wiley-VCH, Weinheim, 2001, pp. 127–132.
- Chantikul, P., Anstis, G. R., Lawn, B. R. and Marshall, D. B., A critical evaluation of indentation techniques for measuring fracture toughness: II, strength method. *J. Am. Ceram. Soc.*, 1981, **64**(9), 539–543.
- Cook, R. F. and Lawn, B. R., A modified indentation toughness technique. *J. Am. Ceram. Soc.*, 1983, **66**(11), C200–C201.
- Li, C.-W., Lee, D.-J. and Lui, S.-C., R-Curve behavior and strength for in-situ reinforced silicon nitrides with different microstructures. *J. Am. Ceram. Soc.*, 1992, **75**(7), 1777–1785.
- Zeng, K., Breder, K. and Rowcliffe, D., Comparison of slow crack growth behavior in alumina and SiC-whisker-reinforced alumina. *J. Am. Ceram. Soc.*, 1993, **76**(7), 1673–1680.
- Ramachandran, N. and Shetty, D. K., Prediction of indentation-load dependence of fracture strengths from R-curves of toughened ceramics. *J. Mater. Sci.*, 1993, **28**, 6120–6126.
- Krause, R. F., Flat and rising R-curves for elliptical surface cracks from indentation and superposed flexure. *J. Am. Ceram. Soc.*, 1994, **77**(1), 172–178.
- Xu, H. H. K., Ostertag, C. P. and Krause, R. F., Effect of temperature on toughness curves in alumina. *J. Am. Ceram. Soc.*, 1995, **78**(1), 260–262.
- Smith, S. M. and Scattergood, R. O., Determination of short-crack toughness curves. *J. Am. Ceram. Soc.*, 1996, **79**(1), 129–136.
- Griggs, J. A., Hill, T. J. and Mecholsky, J. J., A modified flaw-size toughness technique. *Ceram. Eng. Sci. Proc.*, 1999, **20**(3), 393–400.
- Lube, T., Indentation crack profiles in silicon nitride. *J. Eur. Ceram. Soc.*, in press.
- Rice, R. W., Ceramic fracture features, observations, mechanisms, and uses. In *Fractography of Ceramic and Metal Failures*, ed. J. J. Mecholsky, Jr. and S. R. Powell, Jr. ASTM. Spec. Tech. Publ., No. 827, 1984, pp. 5–103.

17. Cook, R. F., Segregation Effects in the Fracture of Brittle Materials: Ca–Al₂O₃. *Acta Metall. Mater.*, 1990, **38**, 1083–1100.
18. Lawn, B. R., *Fracture of Brittle Solids*, 2nd edn. Cambridge Solid State Science Series, Cambridge University Press, Cambridge, 1993 pp. 106–136.
19. Kovar, D. and Readey, M. J., Grain size distributions and strength variability of high-purity alumina. *J. Am. Ceram. Soc.*, 1996, **79**(2), 305–312.
20. Tatami, J., Yasuda, K., Matsuo, Y. and Kimura, S., Stochastic analysis on crack path of polycrystalline ceramics on the difference between the released energies in crack propagation. *J. Mater. Sci.*, 1997, **32**, 2341–2346.
21. Cook, R. F. and Pharr, G. M., Mechanical properties of ceramics. In *Materials Science and Technology, A Comprehensive Treatment, Vol. 11. Structure and Properties of Ceramics*, ed. M. Swain. VCH, New York, 1994, pp. 353–380.
22. Zeng, K., Breder, K. and Rowcliffe, D., Dynamic fatigue of an Al₂O₃/SiC whisker composite in water. *Ceram. Eng. Sci. Proc.*, 1991, **12**(9–10), 2233–2250.
23. Zeng, K. and Rowcliffe, D., Identification of fracture sequences during sharp indentation of polycrystalline Al₂O₃. *J. Mater. Res.*, 1994, **9**(7), 1693–1700.
24. Salomonsson, J. and Rowcliffe, D., Influence of loading rate on transgranular and intergranular fracture in polycrystalline alumina. In *Indentation Fracture of Alumina and Glass*. Thesis, Royal Institute of Technology, Stockholm, 1996.
25. Fett, T., Keller, K., Munz, D. and Kübler, J., Subcritical surface crack growth in borosilicate glass under thermal fatigue. *Theor. Appl. Fract. Mech.*, 1991, **16**, 27–34.
26. Saadaoui, M., Olagnon, C. and Fantozzi, G., Thermal fatigue of alumina: comparison with mechanical data and life time prediction. *Ceram. Int.*, 1999, **25**, 497–504.
27. Ishihara, S., Goshima, T., Nomura, K. and Yoshimoto, T., Crack propagation behavior of cermets and cemented carbides under repeated thermal shocks by the improved quench test. *J. Mater. Sci.*, 1999, **34**, 629–636.
28. Lee, W. J. and Case, D. E., Cyclic thermal shock in SiC-whisker-reinforced alumina composite. *Mater. Sci. Eng.*, 1989, **A119**, 13–126.
29. Anstis, G. R., Chantikul, P., Lawn, B. R. and Marshall, D. B., A critical evaluation of indentation techniques for measuring fracture toughness: i, direct crack measurements. *J. Am. Ceram. Soc.*, 1981, **64**(9), 533–538.
30. Suresh, S., *Fatigue of Materials*. Cambridge University Press, Cambridge, 1991 pp. 403–456.
31. Ritchie, R. O., Mechanisms of fatigue crack propagation in metals, ceramics and composites: role of crack tip shielding. *Mater. Sci. Eng.*, 1988, **A103**, 15–28.
32. Lewis, D. and Rice, R. W., Comparison of static, cyclic, and thermal-shock fatigue in ceramic composites. *Ceram. Eng. Sci. Proc.*, 1982, **3**(9/10), 714–721.
33. Salomonsson, J. and Rowcliffe, D., A study of the velocity of indentation radial cracks in polycrystalline alumina. *Phil. Mag. A*, 1996, **74**(5), 1265–1272.
34. Lawn, B. R., *Fracture of Brittle Solids. Cambridge Solid State Science Series*, 2nd edn. Cambridge University Press, Cambridge, 1993 194–202.
35. Hansson, T., Warren, R. and Wasén, J., Quantitative characterization of toughening mechanisms in alumina and alumina composites. *J. Hard Mater.*, 1993, **4**, 149–165.
36. Becher, R. F., Hsueh, C-H., Alexander, K. B. and Sun, E. Y., Influence of reinforcement content and diameter on the r-curve response in SiC-whisker-reinforced alumina. *J. Am. Ceram. Soc.*, 1996, **79**(2), 298–304.